Desalination and Water Treatment
www.deswater.com

doi: 10.5004/dwt.2019.23325

141 (2019) 115–123
February

Poly(acrylic acid)/SiO_2 composite nanofiber functionalized with mercapto groups for the removal of humic acid from aqueous solution

M.A. Zulfikar[a,*], D. Maulina[a], M. Nasir[b], A. Alni[c], M. Zunita[d], I.S. Zen[e], H. Setiyanto[a], H. Rusli[a]

[a]*Analytical Chemistry Research Group, Institut Teknologi Bandung, Jl. Ganesha 10 Bandung, Indonesia 40132, Tel. +62-22-2502103, email: zulfikar@chem.itb.ac.id (M.A. Zulfikar), dy.maulinayunus@gmail.com (D. Maulina), henry@chem.itb.ac.id (H. Setiyanto), handajaya@chem.itb.ac.id (H. Rusli)*
[b]*Clean Technology Division, Indonesian Institute of Sciences, Jl. Cisitu Lama 1 Bandung, Indonesia 40132, email: mnasir71@yahoo.com (M. Nasir)*
[c]*Organic Chemistry Research Group, Institut Teknologi Bandung, Jl. Ganesha 10 Bandung, Indonesia 40132, email: alni@chem.itb.ac.id (A. Alni)*
[d]*Chemical Engineering Product Design and Development Research Group, Institut Teknologi Bandung, Jl. Ganesha 10 Bandung, Indonesia 40132, email: m.zunita@che.itb.ac.id (M. Zunita)*
[e]*Department of Urban and Regional Planning, Universiti Teknologi Malaysia, Skudai, Johor Bahru, Malaysia 81310, email: irinasafitri@utm.my (I.S. Zen)*

Received 30 April 2018; Accepted 19 October 2018

ABSTRACT

Functionalized poly(acrylic acid)/SiO_2 (PAA/SiO_2) composite nanofiber with mercapto groups have been prepared through an electro spinning process. The characterization of the composite nanofiber was performed using FTIR, optical microscopy, SEM, TEM and Brunauer-Emmett-Teller (BET) analysis. Finally, the prepared nanofiber was used for the adsorption of humic acid (HA) from an aqueous solution using a batch adsorption technique. The effects of pH, contact time, initial concentration, dosages and temperature on adsorption capacities were studied in a batch mode. The experimental data was well described by the Langmuir isotherm model with an adsorption capacity of 427.62 mg/g. It was found that the kinetic data follow the pseudo-second-order models. The data of thermodynamic parameters indicated that the HA adsorption process was non-spontaneous and endothermic under the experimental conditions with the values of Gibbs free energy ($\Delta G°$) being in the range of 3.235 to 5.914 kJ mol^{-1}; as well as the values of enthalpy ($\Delta H°$) and entropy ($\Delta S°$) that were found to be 22.41 kJ mol^{-1} and 55.59 J mol^{-1}. K^{-1}, respectively. The functionalized composite nanofiber exhibited as a high potential adsorbent for the adsorption of HA from an aqueous solution.

Keywords: Adsorption; Composite nanofiber; Humic acid; Mercapto groups

1. Introduction

Humic acid (HA) is a complex product of decomposing plants, and is usually acidic in nature [1,2]. The HA molecules in water can result in a yellowish or brown colour, taste and odor, and can react with disinfectants to produce harmful molecules called disinfectant by-products (DBPs) [2–12], which harmful to human health. Thus, it is very important to remove HAs from water or an aqueous solution.

There are several methods for removing HAs from aqueous solution, including electro coagulation [6], photo catalytic degradation [7], biofiltration [13], biosorption [3], membrane technologies [5,14] and ion-exchange [15,16]. However, these techniques have some disadvantages, such as excessive time requirements, high costs and high energy consumption [11,12]. The adsorption process is an alternative technique for removing HAs from aqueous solutions. Some materials

*Corresponding author.

have been used as adsorbents, such as: activated carbons [1,2,17], cellulose [2], molecularly imprinted polymers [8,11], Fe_3O_4 [9], Fe_3O_4-chitosan hybrid [10], eggshell [12], modified zeolite [4,17], bentonite [18], silica [19], TiO_2 [20] and other adsorbents [21,22]. However, most of these absorbent materials, especially for powder-like absorbents, have several disadvantages such as low adsorption efficiency and uncomfortable use, which has great difficulty in recycling [22]. Therefore, it is important to develop a new high-efficiency adsorbent to remove HA from aqueous solutions.

Some organic/inorganic composite materials may be used as potential adsorbents for the removal of pollutants from an aqueous phase due to their high specific surface area [4,23–25]. This organic/inorganic composite material can be made into a nanofiber form, which facilitates regeneration. In order to increase the adsorption capacity of these nanofiber materials, the following methods have attracted the most attention: (1) surface modification with functional groups and (2) increasing the surface area of nanofibers [26–28]. The nanofibers modified by functional groups have attracted much attention because of their properties such as: (1) high surface-to-volume ratio, (2) uniform pore size distribution, (3) convenient recycling, and (4) high equilibrium adsorption capacities [28]. One functional group that is widely used to modify the adsorbents is marcapto (-SH) [24,28,29,30], because the sulfur atom of the –SH group can form the chelates with the analyte, especially heavy metal ions [28]. Several organic/inorganic composite nanofibers have been modified using marcapto functional groups to remove pollutants from water, such as uranium (VI) ion [24], thorium (IV) ion [24], Cd (II) and Ni(II) ions [30]. However, until now, there has been no study of HA adsorption using composite nanofiber functionalized with marcapto groups.

The aim of this study is to synthesize the PAA/SiO_2 composite nanofiber functionalized with marcapto groups using 3-mercaptopropyltrimethoxylane (TMPTMS) by electro-spinning process and its application as an adsorbent for the adsorption of HA from an aqueous solution. Also, the effects of pH, contact time, adsorbent dosages and temperature in the sorption process were investigated. In addition, the nature of the adsorption process was also studied in batch systems against kinetic, equilibrium and thermodynamic parameters.

2. Materials and methods

2.1. Materials

Poly acrylic acid (PAA) 35% (MM = 240,000 g/mol), 3-mercaptopropyltrimethoxylane (TMPTMS) (MM = 196.34 g/mol), tetraethyl orthosilica (TEOS), cetyltrimethyl ammonium bromide (CTAB), ethanol and hydrochloric acid were purchased from Merck (USA). All materials were used as received without further purification. Deionized water was used in all experiments.

2.2. Preparation of PAA/SiO_2 and PAA/SiO_2/TMPTMS solutions

A solution of mercapto groups functionalized with PAA/SiO_2 for the electro spinning process was prepared by the following procedures. First, a 20% wt PAA solution was prepared by dissolving 6.567 g of PAA in 10 ml of deionized water. For the preparation of a PAA/TiO_2/TMPTMS solution, a 25 wt.% CTAB solution was first prepared by dissolving 0.5 g of CTAB in 2 ml of ethanol and then sonicated for 15 min at 50°C. After that, 2 ml of TEOS and 0.5 ml of TMPTMS were added drop wise to the solution and then sonicated for 30 min at 50°C to obtain a homogeneous solution. During the reaction, 2 M of HCl solution was applied drop wise and sonicated continuously at 50°C until a sol was formed. Finally, 10 ml of a 20wt% PAA solution was added and sonicated continuously for 18 h.

For comparison, the PAA/SiO_2 gel without mercapto functionalized groups was also prepared in a manner similar to the above mentioned method using 2.5 m of TEOS without TMPTMS in the second step.

2.3. Preparation of PAA/SiO_2 and PAA/SiO_2/TMPTMS composite nanofibers

In order to produce nanofibers, each of the above homogenous solutions was put in a plastic syringe with a needle diameter of 0.6 mm. The as-prepared solutions were then electro spun under a fixed voltage of 22 kV. The feeding rate of the polymer solution was 0.005 ml/min and the distance from the tip to the aluminium foil collector was 15 cm. The nanofiber were separated from the surface collector, dried to remove moisture, and used for further analysis and application.

2.4. Characterization studies

The composite nanofibers were examined by FTIR model 8300 IR-TF (Shimadzu, Japan) in the wave number range of 4000–400 cm^{-1}. The surface morphology of the composite nanofiber was investigated using a scanning electron microscopy (SEM) (JSM-6360 LV, Japan) and transmission electron microscopy (TEM) (Hitachi H-600-II, Japan). The surface area of the PAA/SiO_2 and PAA/SiO_2/TMPTMS composite nanofibers was measured using the Brunauer-Emmett-Teller (BET) analyzer (Micromeritics Gemini III 2375, USA). The pore size distributions were calculated using the Barret-Joyner-Halenda (BJH) model by means of a porosimeter (Autoporel V 9500, Micromeritics Co., USA).

2.5. Adsorption studies

The adsorption experiment was carried out by mixing 0.01 g of composite nanofiber with 25 ml of HA solution in a flask. The effect of pH on the sorption of HA was studied in the range of 2–12, at the contact time of 2 h and 25°C. The effect of the agitation time on the adsorption capacity of the adsorbent was investigated by varying the time from 0 to 200 min, at an optimum pH and 25°C. The effect of the initial HA concentration was studied in the range of 10–300 mg/l, at 25°C and at optimum contact time. The effect of the adsorbent dose on the adsorption capacity was studied in the range of 0.005–0.05 g in 25 ml of HA solution at an optimum contact time and pH and 25°C. The effect of temperature on HA adsorption was studied by performing experiments at 25, 45, 60 and 75°C at optimum contact time,

pH and dose. The concentration of HA solution before and after adsorption was determined using an ultraviolet-visible spectrophotometer model UV-Vis 1601 (Agilent 8453, USA) at the l 254 nm [8,11]. The percentage adsorption of HA was calculated using the following equation:

$$\%\ \text{Adsorption} = \frac{C_i - C_e}{C_i} \times 100 \quad (1)$$

where C_i and C_e are the initial and final concentrations of HA (mg·L^{-1}) in solution, respectively. The adsorbent adsorption capacity in a system with the volume of solution V (L) is expressed as:

$$q_e\left(\text{mg.g}^{-1}\right) = \frac{C_i - C_e}{m} \times V \quad (2)$$

where C_i and C_e are the initial and final concentrations of HA (mg·L^{-1}) in solution, respectively and m is the mass of the adsorbent (g) used.

3. Results and discussion

3.1. Adsorbent characterization

The FTIR spectra of functional groups of pure PAA nanofibers, PAA/SiO_2 and PAA/SiO_2/TMPTMS composite nanofibers are shown in Fig. 1. The broad band was observed from 3100 to 3600 cm^{-1} in pure PAA nanofiber corresponding to –OH stretching. The characteristic bands of 2849, 2916 and 1420 cm^{-1} are attributed to the stretching vibrations of the C-H and C-O bonds, respectively.

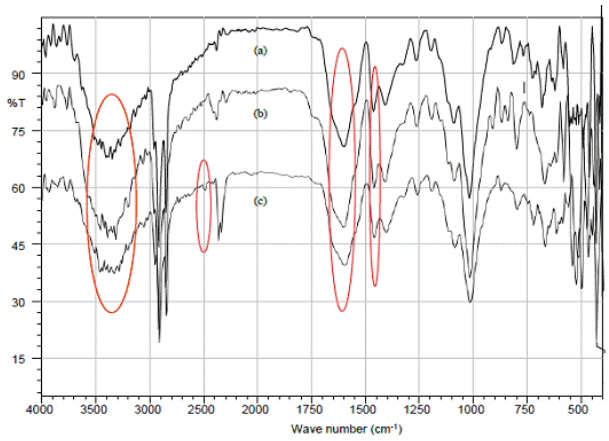

Fig. 1. FTIR spectrum of (a) PAA, (b) PAA/SiO_2 and (c) PAA/SiO_2/TMPTMS nanofiber adsorbents.

The band observed at 1600 cm^{-1} is caused by the functional groups of C=O. A new broadband of about 800–1300 cm^{-1} was observed in both PAA/SiO_2 and PAA/SiO_2/TMPTMS composite nanofiber due to the Si-O-Si stretching vibration. For PAA/SiO_2/TMPTMS composite nanofiber, the weak bands observed at 2557 cm^{-1} are related to the –SH stretching, which indicates that the mercapto group has been successfully inserted into the nanofiber.

The surface morphology of pure PAA nanofiber, PAA/SiO_2 and PAA/SiO_2/TMPTMS composite nanofibers was explored by scanning electron microscopy (SEM), as shown in Fig. 2. The morphology of pure PAA nanofiber is shown in Fig. 2a. As shown in Fig. 2a, the surface of the pure PAA nanofiber is compact and smooth. SEM image of PAA/SiO_2 composite nanofiber is shown in Fig. 2b. The SEM image clearly shows that the nanofiber has ultra fine fibers with an average diameter of 382 nm. The SEM images of PAA/SiO_2/TMPTMS composite nanofibers are given in Fig. 2c. As can be seen in Fig. 2c, the perfect uniform fibers without any drops and beads were obtained. From Fig. 2c, it was also shown that the diameter of the PAA/SiO_2/TMPTMS composite nanofiber obtained is smaller than the diameter of the PAA/SiO_2 composite nanofiber. This observation is similar to that reported by other researchers [24].

The characteristics of pure PAA nanofiber, PAA/SiO_2 and PAA/SiO_2/TMPTMS composite nanofibers are shown in Table 1. It can be seen from Table 1 that the surface area, the average pore diameter and the pore volume of PAA/SiO_2/TMPTMS composite nanofibers are greater than both pure PAA and PAA/SiO_2 composite nanofibers. However, in comparison with some other SiO_2 composite mesoporous materials reported [23,25,30], the PAA/SiO_2/TMPTMS composite nanofiber synthesized in this study possessed a relatively lower specific surface area.

3.2. Adsorption studies

3.2.1. Effect of contact time

The adsorption percentage of HA on both PAA/SiO_2 and PAA/SiO_2/TMPTMS composite nanofibers is plotted

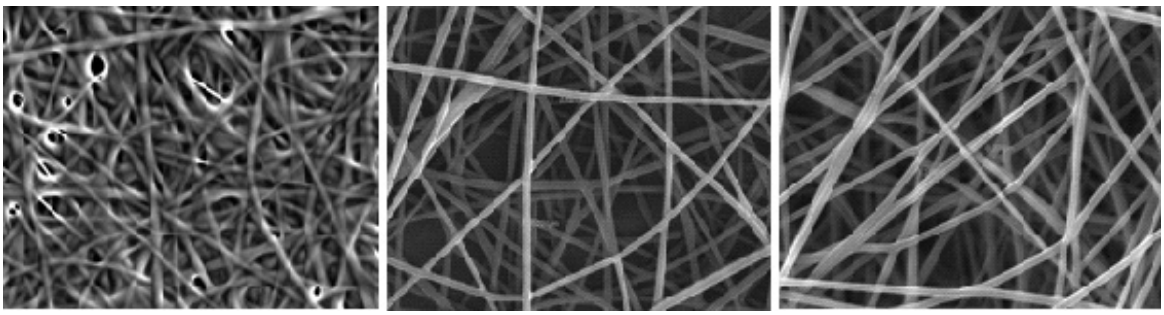

(A) (B) (C)

Fig. 2. SEM images of (a) PAA, (b) PAA/SiO_2 and (c) PAA/SiO_2/TMPTMS nanofiber adsorbents.

Table 1
Physical properties of PAA, PAA/SiO_2 and PAA/SiO_2/TMPTMS nanofiber adsorbents

Parameters	PAA	PAA/SiO_2	PAA/SiO_2/TMPTMS
BET surface area (m^2/g)	53.38	87.76	108.54
Average diameter (nm)	681	382.5	246
Average pore diameter (nm)	3.28	3.76	4.28
Pore volume (cm^3/g)	0.412	0.475	0.627

in Fig. 3 as a function of the adsorption time. Within the first forty minutes, the adsorption percentage of HA increased sharply. After that, the amount of adsorption leveled off and gradually reached equilibrium. This is due to the high availability in a series of active sites on the surface of the adsorbent in the early stages.

From Fig. 3, we can also observe that the adsorption percentage of HA using the PAA/SiO_2/TMPTMS composite nanofiber is higher than that of the PAA/SiO_2 composite nanofiber for the same agitation time period. This result demonstrates the effect of the mercapto groups of the PAA/SiO_2/TMPTMS composite nanofiber for the HA adsorption.

3.2.2. Effect of pH

pH is one of the important parameters for controlling the adsorption in water-adsorbent interfaces. The effect of pH on the adsorption percentage of HA of the PAA/SiO_2/TMPTMS composite nanofiber is shown in Fig. 4. From Fig. 4, it can be seen that the adsorption percentage of HA of the PAA/SiO_2/TMPTMS composite nanofiber increases with increasing pH of the solution and reaches a maximum at pH 4.0, and then decreases with increasing pH values.

The pH effect on the adsorption of HA can be explained by electrostatic mechanisms. HA molecules mostly contain carboxyl and phenolic functional groups that contribute to the overall molecular charge of HA. At pH < 4, the adsorbent surface is positively charged due to the protonation of the silane and mercapto groups [24,29,30], while the overall charge of the HA macromolecules becomes less negative, resulting in electrostatic repulsion that leads to decreased adsorption of HA.

At pH > 4.0, the surface of PAA/SiO_2/TMPTMS composite nanofiber becomes less positive, while the hydrophilic functional groups of HA deprotonates and the overall charge of an HA macromolecule become more negative. This results in an increase in repulsion between HA and composite nanofiber, thus causing a decrease in the adsorptivity of HA. In addition, at high pH, there exist a fairly linear or stretched structure [4], resulting in an increase in the size of HA macromolecules and causes less adsorption of HA on the adsorbent surface.

3.2.3. Effect of dose

The adsorbent dose is an important parameter in the adsorption process, since it is related to the adsorption capacity of an adsorbent. Fig. 5 shows the effect of the adsorbent dose on adsorption percentage of HA at 25°C and at pH 4.0. From Fig. 5, it can be seen that initially the adsorption percentage of HA increased with increasing adsorbent dose, which was attributed to an increased surface area and availability of more adsorption sites on the PAA/SiO_2/TMPTMS composite nanofiber. Above a dose of

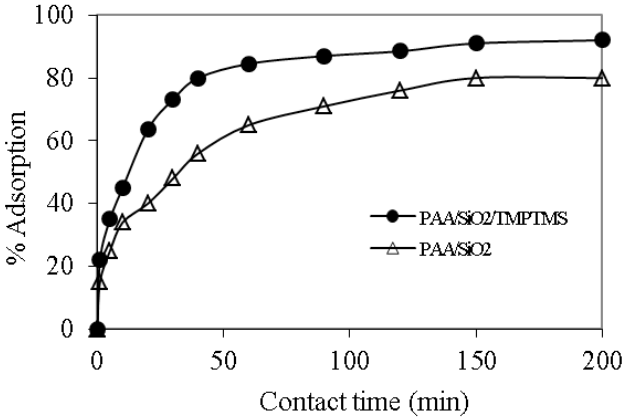

Fig. 3. Effect of contact time on HA adsorption from aqueous solution.

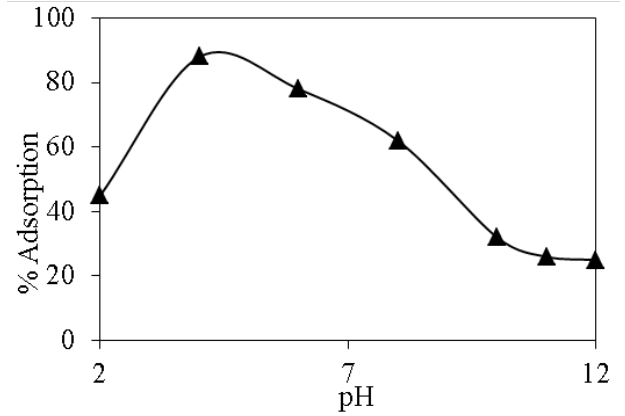

Fig. 4. Effect of pH on HA adsorption from aqueous solution.

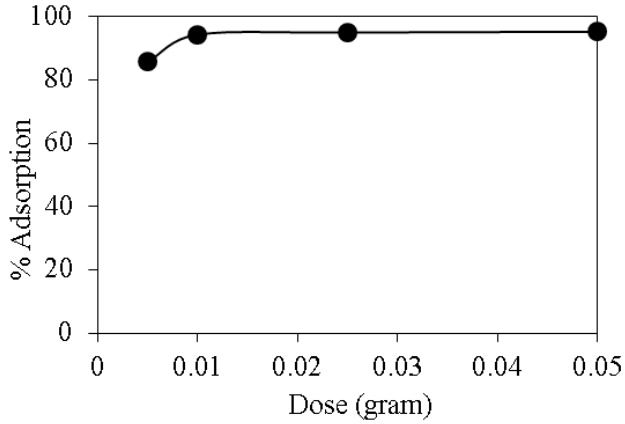

Fig. 5. Effect of adsorbent dose on HA adsorption from aqueous solution.

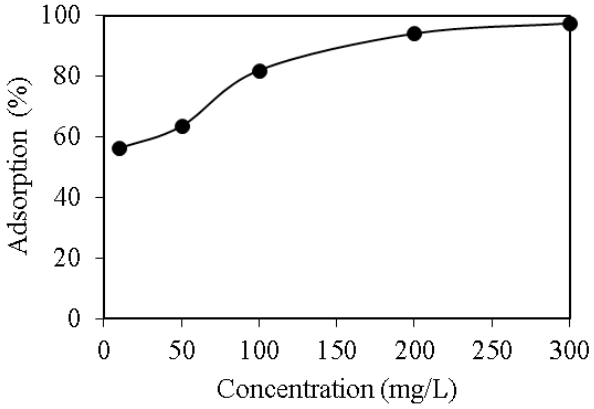

Fig. 6. Effect of initial concentration on HA adsorption from aqueous solution.

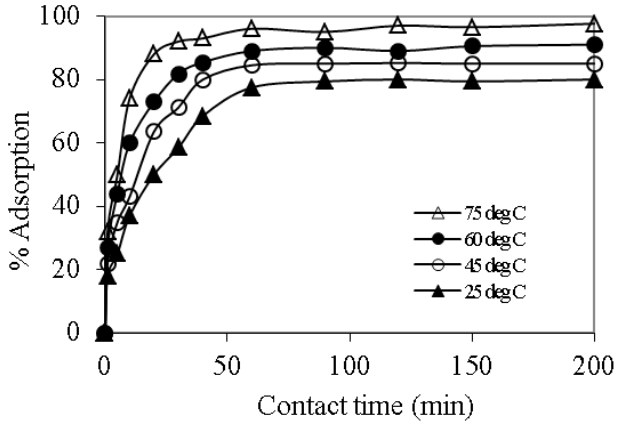

Fig. 7. Effect of temperature on HA adsorption from aqueous solution.

0.01 g adsorbent, the adsorption percentage increase of HA is small and negligible. Therefore, 0.01 g was chosen as the adsorbent dose for all adsorption experiments.

3.2.4. Effect of initial concentration

The initial concentration provides a driving force to overcome all the mass transfer resistance of the adsorbate between the aqueous and the solid phase [2,9,10,17,21], which affects the rate of adsorbate molecule in the solution [2]. Fig. 6 shows that the adsorption percentage of HA of PAA/SiO_2/TMPTMS composite nanofiber increased from 56.31 to 97.48% at 25°C with increasing initial concentration of HA. This is because at low initial concentrations of HAs, the adsorbent sites available in the adsorbents are easily occupied by HA molecules. Conversely, with an initial increase in HA concentrations, most of the available adsorption sites become occupied, and thus the adsorption capacity becomes fixed.

3.2.5. Effect of temperature

Fig. 7 shows that as the temperature of the solution increases, the adsorption percentage of HA also increases. This indicates that favorable adsorption occurs at higher temperatures. The phenomenon may be due to the increase in the diffusion rate and the mobility of the HA molecules through the surface of the adsorbent. In other words, by increasing the temperature, the HA adsorption percentage of PAA/SiO_2/TMPTMS composite nanofiber can be increased. In addition, an increase in temperature also causes swelling in the internal structure of the adsorbent, thereby facilitating the penetration of HA molecules into the adsorbent [8,12]. This indicates that the adsorption of HA into the PAA/SiO_2/TMPTMS adsorbent nanofiber is controlled by an endothermic process.

3.2.6. Adsorption isotherm

The adsorption isotherm describes the relationship between the amount of solute adsorbed on the adsorbent and the amount of solute remaining in the solution at equilibrium. In this case, the Langmuir and Freundlich models were used to describe the adsorption of HA on the PAA/SiO_2/TMPTMS composite nanofiber. The Langmuir model was used to describe the adsorption of a sorbate on a homogeneous surface of an adsorbent, and each adsorptive site can only be occupied by one molecule of adsorbate. The Freundlich adsorption equation was used to describe experimental adsorption data based on empirical equations that are used to describe multilayer adsorption on a heterogeneous surface. The non-linear Langmuir model equations can be expressed as follows:

$$q_e = \frac{q_m \cdot b \cdot C_e}{1 + b \cdot C_e} \tag{3}$$

The Freundlich equation can be written as:

$$q_e = K_f C_e^{\,1/n} \tag{4}$$

where C_e represents the equilibrium concentration (mg·L^{-1}), q_e and q_m represent the amount adsorbed per amount of absorbent at the equilibrium and at maximum (mg·g^{-1}), respectively, b is the Langmuir constant (L·mg^{-1}). K_f (mg·g^{-1}) and n are Freundlich parameters related to the sorption capacity and the sorption intensity of the adsorbent.

Fig. 8 shows the Langmuir and Freundlich isotherm curves for the adsorption of HA on PAA/SiO_2/TMPTMS composite nanofiber and its adsorption isotherm parameters are shown in Table 2. Table 2 shows that the correlation coefficient of Langmuir isotherm is higher than Freundlich isotherm, indicating that the HA adsorption on the PAA/SiO_2/TMPTMS composite nanofiber follows the Langmuir model, with maximum monolayer HA adsorption capacity of 427.62 mg/g.

The essential feature of the Langmuir isotherm can be expressed in terms of a dimensionless constant separation factor, R_L [2,4,18,24], which is expressed as:

$$R_L = [1/(1+b \cdot C_o)] \tag{5}$$

The R_L value is classified into 3 categories: $R_L = 0$, $0 < R_L < 1$, and $R_L > 1$, indicating that the adsorption is irreversible, favorable, and unfavorable, respectively [2,4,18,24].

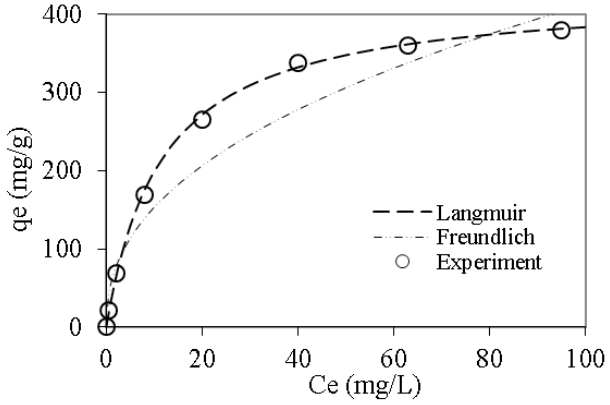

Fig. 8. Isotherm curve for HA adsorption from aqueous solution.

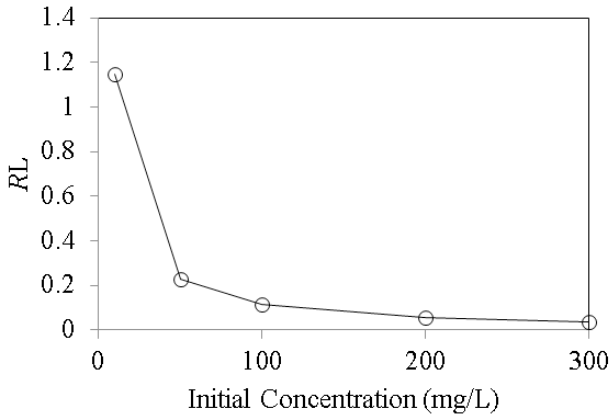

Fig. 9. R_L for the adsorption of HA onto PAA/SiO_2/TMPTMS nanofiber adsorbents.

Table 2
Langmuir and Freundlich parameters for HA adsorption onto PAA/SiO_2/TMPTMS nanofiber adsorbents

Langmuir Model			Freundlich Model		
b (L·mg^{-1})	q_m (mg·g^{-1})	R^2	n	K_f (mg·g^{-1})	R^2
0.09	427.62	0.997	2.33	56.92	0.883

Fig. 9 shows the relationship between the R_L values with the initial concentration of HA. From Fig. 9, it can be seen that as the initial concentration of HA increases, the R_L value decreases. This shows that HA adsorption on the PAA/SiO_2/TMPTMS composite nanofiber was more favorable at higher initial HA concentrations.

3.2.7. Adsorption kinetics

Adsorption kinetics is an important parameter for determining the rate and mechanism of reactions. In order to investigate the adsorption kinetics of HA on the PAA/SiO_2/TMPTMS composite nanofiber, three different kinetics models, pseudo first-order and pseudo second-order rate models as well as intra-particle diffusion models, were used in this study. The linearized form of the pseudo first-order kinetics equation is shown in Eq. (6):

$$\log (q_e - q_t) = \log q_e - (k_1/2.303)\, t \quad (6)$$

where q_e and q_t are the adsorption capacity (mg/g) at equilibrium and at time, t (min), respectively, and k_1 (min^{-1}) is the Lagergren rate constant of adsorption. The rate constant k_1 and q_e were determined from the intercept and the slope of a plot of log ($q_e - q_t$) vs. t.

The pseudo-second-order kinetic model was also analyzed to fit the data and is given by:

$$t/q_t = 1/k_2 \cdot q_e^{\,2} + t/q_e \quad (7)$$

where k_2 (g mg^{-1} min^{-1}) is the pseudo-second-order rate constant of adsorption. The values of k_2 and q_e can be obtained from the intercept and the slope of the linear plot of (t/q_t) vs. t.

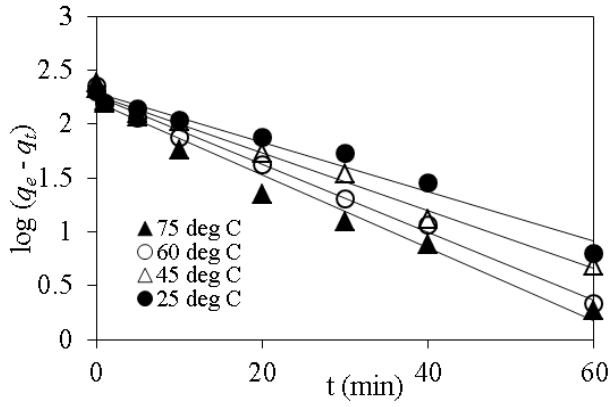

(a)

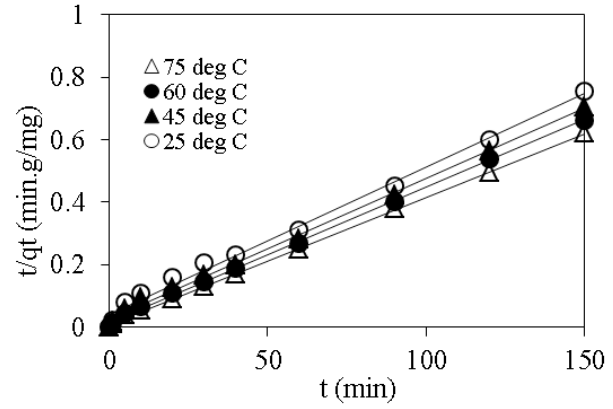

(b)

Fig. 10. Pseudo-first order (a) and pseudo-second order (b) plots for HA removal from aqueous solution.

From Fig. 10 it was observed that the pseudo-second-order kinetic model adequately fit the experimental values. In addition, the value of q_e calculated by the pseudo-second-order model is closer to the experimental value than the pseudo-first-order model (Table 3). These

Table 3
The pseudo-first-order and second-order kinetics parameters for HA adsorption from aqueous solution using PAA/SiO_2/TMPTMS nanofiber adsorbents

Temperature	Pseudo-first-order			Pseudo-second-order			
(°C)	k_1 (min^{-1})	q_e, cal (mg/g)	R^2	k_2 (g $mg^{-1}min^{-1}$)	q_e, cal (mg/g)	R^2	q_e, exp (mg/g)
25	0.0525	194.40	0.972	0.0005	212.77	0.993	210.25
45	0.0617	186.94	0.991	0.0007	227.27	0.997	223.12
60	0.0728	180.88	0.993	0.0012	232.56	0.999	235.16
75	0.0781	161.03	0.974	0.0018	243.90	0.998	242.50

results suggest that HA adsorption on the PAA/SiO_2/TMPTMS composite nanofiber follows the pseudo-second-order kinetic model.

The intra-particle diffusion model can be defined as:

$$q_t = k_d \cdot t^{1/2} + C \quad (8)$$

where k_d is the diffusion rate constant ($mg \cdot g^{-1} \cdot min^{-1/2}$). The value of k_d can be determined from the slope of the straight line.

Fig. 11 shows the Weber and Morris plots for HA adsorption at all temperatures used. As can be seen from Fig. 11, the plots show two linear portions. The first portion relates to the boundary layer diffusion (film diffusion), and the slope of the second linear portion is the rate constant for intra particle diffusion. Fig. 11 also shows that the plot of q_t vs. $t^{1/2}$ does not pass through the origin, which indicates that the adsorption process of HA is not controlled only by intra-particle diffusion [2,4,8,11].

The kinetic parameters calculated from the diffusion kinetic models are listed in Table 4. Both k_{d1} and k_{d2} values were found to increase with increasing temperature. This indicates that increasing temperature increases the migration of HA to the PAA/SiO_2/TMPTMS composite nanofiber.

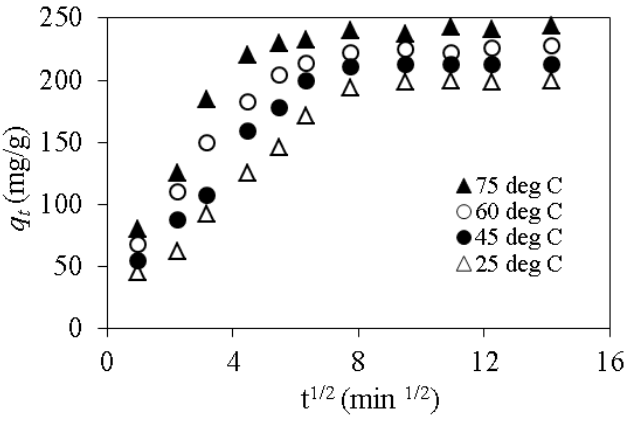

Fig. 11. Plots of intra-particle diffusion model for HA removal from aqueous solution.

Table 4
Parameter of the intra-particle diffusion model for for HA adsorption onto PAA/SiO_2/TMPTMS nanofiber adsorbents

Temperature (°C)	k_{d1} ($mg \cdot g^{-1} \cdot min^{-1/2}$)	R^2	k_{d2} ($mg \cdot g^{-1} \cdot min^{-1/2}$)	R^2
25	0.3877	0.992	0.0024	0.720
45	0.4468	0.992	0.0126	0.684
60	0.4946	0.985	0.0232	0.700
75	0.6705	0.976	0.0236	0.802

3.2.8. Thermodynamic adsorption

Thermodynamic parameters play an important role in adsorption process, which determines the degree of the spontaneous process. The thermodynamics of HA sorption on the PAA/SiO_2/TMPTMS composite nanofiber was evaluated using the following equations:

$$\Delta G^o = -RT \ln b \quad (9)$$

$$\ln b = \frac{\Delta S^o}{R} - \frac{\Delta H^o}{R \cdot T} \quad (10)$$

where R and b (L/mg) are the gas constant and the Langmuir isotherm constant, respectively and T is the absolute temperature. The thermodynamic parameters (ΔG^o, ΔH^o and ΔS^o) are shown in Table 5.

The positive $\Delta G°$ value at all temperatures confirms the endothermic and non-spontaneous nature of the adsorption process, while the positive $\Delta H°$ value indicates that the adsorption process is endothermic in nature. From Table 5, ΔS^o value was also observed to be positive, indicating the increased randomness in the solid (adsorbent)-HA solution interface during the adsorption and also reflects a high affinity adsorbent of HA molecules [4,9–11,24,25].

3.2.9. Activation energy

Generally, an increase in the temperature of a chemical reaction increases the rate of the reaction, and the temperature dependence results in a change in the rate

Table 5
Thermodynamic parameters for the HAs adsorption onto PAA/SiO_2/TMPTMS nanofiber adsorbents

Temperature (°C)	b (L/mg)	ΔG^o (kJ/mol)	ΔH^o (kJ/mol)	ΔS^o (J/mol.K)
25	0.092	5.914		
45	0.172	4.656	22.41	55.59
60	0.264	3.688		
75	0.327	3.235		

constant. The relationship between the reaction rate and temperatures is given in the Arrhenius equation:

$$\ln k = \ln A - \frac{E_a}{R \cdot T} \quad (11)$$

where k is rate constant for sorption (g·min^{-1}), E_a is the activation energy (kJ/mol), A is the Arrhenius factor, R is the gas constant (8.314 J/mol K) and T is the absolute temperature of the solution (K). In this study, the activation energy of the sorption process was calculated using the values of the rate constant from a pseudo-second-order kinetic equation at four different temperatures. The linear plot of ln k_2 versus $1/T$ gives a straight line with a slope of $-E_a/R$ (figure not shown here). The activation energy obtained in this study was 22.48 kJ/mol. The positive value of E_a indicates that an increase in temperature favors the adsorption of HA on the PAA/SiO_2/TMPTMS composite nanofiber, and that the adsorption process is endothermic in nature [4,8,11].

3.2.10. Regeneration of PAA/SiO_2/TMPTMS composite nanofiber

The regeneration of the adsorbent is very important in the adsorption process, because the reuse of the adsorbent is a key factor in improving process economics [24]. The most common stripping agents used to regenerate adsorbents are NaOH, HCl, HNO_3, EDTA, $CaCl_2$, and organic solvents such as methanol and ethanol [12]. In this study, the stripping agent used was 1 mol/L of HCl at an initial HA concentration of 200 mg/l and 25°C. The results for the cycling and reusability of the PAA/SiO_2/TMPTMS composite nanofiber are shown in Fig. 12. According to Fig. 12, even in five regeneration cycles, the adsorption percentage of HA decreased only from 83.30 to 78.25. This indicates that the adsorption capacity of the PAA/SiO_2/TMPTMS composite nanofiber for HA was almost fully restored, and can be reused frequently with almost no significant loss in adsorption performance.

3.2.11. Comparison of HA removal with other adsorbents reported in literature

It is also important to compare the value of the maximum adsorption capacity obtained from this study with the values from other reported adsorbents, as this would indicate the effectiveness of PAA/SiO_2/TMPTMS composite nanofiber for HA removal. The adsorption capacity values for HA removal using some adsorbents are shown in Table 6.

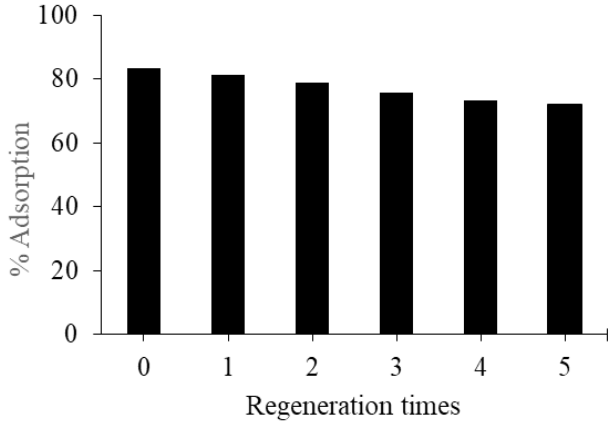

Fig. 12. Removal efficiency of HA on PAA/SiO_2/TMPTMS nanofiber at different regeneration cycles.

Table 6
Comparison of adsorption capacity of various adsorbent for HA removal

Adsorbent(s)	q_m (mg/g)	pH	Reference
Activated carbon	6.9	–	[1]
Activated carbon	30.4	2	[2]
Cellulose	89.3	2	[2]
Chitosan-zeolite composite	74.1	7	[4]
Chitosan-zeolite composite surfactant-modified	164	7	[4]
Molecularly imprinted polymers (MIPs)	45.45	2	[8]
Fe_3O_4	43.32	2	[9]
Fe_3O_4-chitosan hybrid	44.84	4	[10]
Molecularly imprinted polymers (MIPs) nanofiber	153.3	4	[11]
Powder eggshell	126.58	4	[12]
Zinc oxide-coated zeolite	109–120	–	[17]
Bentonite	4.01	–	[18]
SiO_2 particles (100 nm)	165.6	4	[19]
Single wall carbon nanotubes	116	4	[21]
PAA/SiO_2/TMPTMS nanofiber	427.62	4	This study

From Table 6, it was observed that the maximum adsorption capacity at equilibrium of PAA/SiO_2/TMPTMS composite nanofiber adsorbents was better than most other materials in the previous literature studies. It could be used as a promising and effective adsorbent to be used in the drinking water treatment process.

4. Conclusions

In this study, poly(acrylic acid)/SiO_2 (PAA/SiO_2) composite nanofiber functionalized with mercapto groups have been prepared. The composite nanofibers display high adsorption for HA molecules. The HA adsorption capacity

of PAA/SiO_2/TMPTMS composite nanofiber was found to increase with increasing contact time, adsorbent dosage and temperature. The adsorption kinetics of HA on the PAA/SiO_2/TMPTMS composite nanofiber accorded with the pseudo-second-order model. The equilibrium isotherm of these HA was obtained, which was best fitted to the Langmuir isotherm model than the Freundlich isotherm model. Based on the Langmuir isotherm model, the maximum monolayer HA adsorption capacity for PAA/SiO_2/TMPTMS composite nanofiber was 427.62 mg/g. The thermodynamic parameters indicated that the adsorption of HA on the PAA/SiO_2/TMPTMS composite nanofiber was non-spontaneous and endothermic in nature. The results of this work show that PAA/SiO_2/TMPTMS composite nanofiber is a potential adsorbent for its use in the drinking water treatment process.

Acknowledgment

The author is very grateful to the Institut Teknologi Bandung for the financial support of this research study through the ITB Research Program 2018.

References

[1] M.A.F. Garcı´a, J.R. Utrilla, I.B. Toledo, C.M. Castilla, Adsorption of humic substances on activated carbon from aqueous solutions and their effect on the removal of Cr (III) ions, Langmuir, 14 (1998) 1880–1886.
[2] N.T. Tavengwa, L. Chimuka, L. Tichagwa, Equilibrium and kinetic studies on the adsorption of humic acid onto cellulose and powdered activated carbon, Desal. Water Treat., 57(36) (2016) 16843–16854.
[3] F. Hua-Jun, H. Li-Fang, M. Qaisar, L. Yan, S. Dong-Sheng, Study on biosorption of humic acid by activated sludge, Biochem. Eng. J., 39 (2008) 478–485.
[4] J. Lin, Y. Zhan, Adsorption of humic acid from aqueous solution onto unmodified and surfactant-modified chitosan/zeolite composites, Chem. Eng. J., 200–202 (2012) 202–213.
[5] B. Ma, Y. Ding, W. Li, C. Hu, M. Yang, H. Liu, J. Qu, Ultra filtration membrane fouling induced by humic acid with typical inorganic salts, Chemosphere, 197 (2018) 793–802.
[6] F. Ulu, S. Barışçī, M. Koby, H. Särkkä, M. Sillanpää, Removal of humic substances by electro coagulation (EC) process and characterization of floc size growth mechanism under optimum conditions, Sep. Purif. Technol., 133 (2014) 246–253.
[7] X. Wang, Z. Wu, Y. Wang, W. Wang, X. Wang, Y. Bu, J. Zhao, Adsorption-photo degradation of humic acid in water by using ZnO coupled TiO_2/bamboo charcoal under visible light irradiation, J. Hazard. Mater., 262 (2013) 16–24.
[8] M.A. Zulfikar, D. Wahyuningrum, R. Mukti, H. Setiyanto, Molecularly imprinted polymers (MIPs): a functional material for removal of humic acid from peat water, Desal. Water Treat., 57(32) (2016) 15164–15175.
[9] M.A. Zulfikar, F.I. Suri, Rusnadi, H. Setiyanto, N. Mufti, M. Ledyastuti, D. Wahyuningrum, Fe_3O_4 nano-particles prepared by co-precipitation method using local sands as a raw material and their application for humic acid removal, Int. J. Environ. Stud., 73 (2016) 79–94.
[10] M.A. Zulfikar, S. Afrita, D. Wahyuningrum, M. Ledyastuti, Preparation of Fe_3O_4-chitosan hybrid nano-particles used for humic acid removal from aqueous solution, Environ. Nanotechnol. Monit. Manage., 6 (2016) 64–75.
[11] M.A. Zulfikar, I. Afrianingsih, M. Nasir, N. Handayani, Fabrication of nanofiber membrane functionalized with molecularly imprinted polymers for humic acid removal from peat water, Desal. Water Treat., 97 (2017) 203–212.
[12] M.A. Zulfikar, E. Novita, R. Hertadi, S.D. Djajanti, Removal of humic acid from peat water using untreated powdered eggshell as a low cost adsorbent, Int. J. Environ. Sci. Technol., 10 (2013) 1357–1366.
[13] B. Seredynska-Sobecka, M. Tomaszewska, A.W. Morawski, Removal of humic acids by the ozonation-biofiltration process, Desalination, 198 (2006) 265–273.
[14] A. Mehrparvar, A. Rahimpour, M. Jahanshahi, Modified ultra filtration membranes for humic acid removal, J. Taiwan Inst. Chem. Eng., 45 (2014) 275–282.
[15] H. Baker, F. Khalili, Comparative study of binding strengths and thermodynamic aspects of Cu(II) and Ni(II) with humic acid by Schubert's ion-exchange method, Anal. Chim. Acta, 497 (2003) 235–248.
[16] H. Baker, F. Khalili, A study of complexation thermodynamic of humic acid with cadmium (II) and zinc (II) by Schubert's ion-exchange method, Anal. Chim. Acta, 542 (2005) 240–248.
[17] L. Wang, C. Han, M.N. Nadagouda, D.D. Dionysiou, An innovative zinc oxide coated zeolite adsorbent for removal of humic acid. J. Hazard. Mater., 313 (2016) 283–290.
[18] C. Leodopoulos, D. Doulia, K. Gimouhopoulos, T. Triantis, Single and simultaneous adsorption of methyl orange and humic acid onto bentonite. Appl. Clay Sci., 70 (2012) 84–90.
[19] L. Liang, L. Luo, S. Zhang, Adsorption and desorption of humic and fulvic acids on SiO_2 particles at nano- and micro-scales, Colloid Surf. A., 384 (2011) 126–130.
[20] D.D. Sun, P.F. Lee, TiO_2 micro sphere for the removal of humic acid from water: Complex surface adsorption mechanisms, Sep. Purif. Technol., 91 (2012) 30–37.
[21] S.P. Moussavi, M.H. Ehrampoush, A.H. Mahvi, M. Ahmadian, S. Rahimi, Adsorption of humic acid from aqueous solution on single-walled carbon nanotubes, Asian J. Chem., 25 (2013) 5319–5324.
[22] Y. Lu, Z. Wu, M. Li, Q. Liu, D. Wang, Hydrophilic PVA-co-PE nanofiber membrane functionalized with iminodiacetic acid by solid-phase synthesis for heavy metal ions removal, React. Funct. Polym., 82 (2014) 98–102.
[23] R. Xu, M. Jia, Y. Zhang, F. Li, Sorption of malachite green on vinyl-modified mesoporous poly(acrylic acid)/SiO_2 composite nanofiber membranes, Micro porous Mesoporous Mater., 149 (2012) 111–118.
[24] S. Abbasizadeh, A.R. Keshtkar, M.A. Mousavian, Preparation of a novel electro spun polyvinyl alcohol/titanium oxide nanofiber adsorbent modified with mercapto groups for uranium (VI) and thorium (IV) removal from aqueous solution, Chem. Eng. J., 220 (2013) 161–171.
[25] A.R. Keshtkar, M. Irani, M.A. Moosavian, Removal of uranium (VI) from aqueous solutions by adsorption using a novel electro spun PVA/TEOS/APTES hybrid nanofiber membrane: comparison with casting PVA/TEOS/APTES hybrid membrane, J. Radioanal. Nucl. Chem., 295 (2013) 563–571.
[26] Y.J. Qiu, J. Yu, J. Rafique, J. Yin, X.D. Bai, E.G. Wang, Large-scale production of aligned long boron nitride nanofibers by multi jet/multi collector electro spinning, J. Phys. Chem. C., 113 (2009) 11228–11234.
[27] R. Ostermann, D. Li, Y.D. Yin, J.T. McCann, Y.N. Xia, V_2O_5 nanorods on TiO_2 nanofibers: a new class of hierarchical nanostructures enabled by electro spinning and calcination, Nano Lett., 6 (2006) 1297–1302.
[28] S. Wu, F. Li, H. Wang, L. Fu, B. Zhang, G. Li, Effects of poly (vinyl alcohol) (PVA) content on preparation of novel thiol-functionalized mesoporous PVA/SiO_2 composite nanofiber membranes and their application for adsorption of heavy metal ions from aqueous solution, Polymer., 51 (2010) 6203–6211.
[29] X. Xue, F. Li, Removal of Cu(II) from aqueous solution by adsorption onto functionalized SBA-16 mesoporous silica, Micro porous Mesoporous Mater., 116 (2008) 116–122.
[30] M. Irani, A.R. Keshtkar, M.A. Mousavian, Removal of Cd(II) and Ni(II) from aqueous solution by PVA/TEOS/TMPTMS hybrid membrane, Chem. Eng. J., 175 (2011) 251–259.